Stone-Wales defects in graphene and other planar sp^2-bonded materials

Jie Ma,[1,2,3] Dario Alfè,[2,4,5] Angelos Michaelides,[2,3,*] and Enge Wang[1]

[1]*Institute of Physics, Chinese Academy of Sciences, P.O. Box 603, Beijing 100190, China*
[2]*London Centre for Nanotechnology, University College London, London WC1E 6BT, United Kingdom*
[3]*Department of Chemistry, University College London, London WC1E 6BT, United Kingdom*
[4]*Department of Physics and Astronomy, University College London, London WC1E 6BT, United Kingdom*
[5]*Department of Earth Sciences, University College London, London WC1E 6BT, United Kingdom*

Density functional theory and quantum Monte Carlo simulations reveal that the structure of the Stone-Wales (SW) defect in graphene is more complex than hitherto appreciated. Rather than being a simple in-plane transformation of two carbon atoms, out-of-plane wavelike defect structures that extend over several nanometers are predicted. Equivalent wavelike SW reconstructions are predicted for hexagonal boron-nitride and polycyclic aromatic hydrocarbons above a critical size, demonstrating the relevance of these predictions to sp^2-bonded materials in general.

I. INTRODUCTION

Stone-Wales (SW) defects[1] are important topological defects in sp^2-bonded carbon materials, playing a central role in the formation, transformation, fracture, and embrittlement of carbon nanotubes, fullerenes, and other carbon nanostructures.[2–6] SW defects have also been predicted to alter the electronic properties (band structure and density of states) of graphene and in so doing modify its chemical reactivity toward adsorbates, and likely impact upon its unique transport properties.[7–9] Gaining basic knowledge of SW defects in graphene is therefore essential to deepen fundamental understanding of this most interesting of two-dimensional (2D) materials.

SW defects involve an in-plane 90° rotation of two carbon atoms with respect to the midpoint of the bond. In this transformation four hexagons are changed into two heptagons and two pentagons, as shown in Figs. 1(a) and 1(b). It has been predicted that chemically modified SW defects exhibit local out-of-plane displacements of the carbon atoms,[10,11] and it is known that heptagons and pentagons induce curvature in graphitic materials.[12] However, in clean unmodified graphene it is customarily assumed that SW defects are perfect two-dimensional defects. None of the many studies, which have sought to understand the mechanism of their formation, their stability relative to perfect graphene, their electronic properties, and their impact on the strength of graphene, have altered the view that SW defects are simple and local topological defects.[7,8,13–17]

Here we show with density functional theory (DFT) and quantum Monte Carlo (QMC) that the canonical flat SW defect in graphene is in fact not a local minimum on the potential-energy surface (PES). Rather it is a saddle point that separates two lower-energy buckled defect structures. In one, both atoms move out of plane in the same direction. In the other lower-energy structure the defect atoms move out of plane in the opposite direction. The out-of-plane displacements at the defect core lower the energy by allowing the (compressed) C-C bonds in its vicinity to expand. These set up out-of-plane displacement fields in the graphene sheet

that extend to the boundaries of our several nanometer wide simulation cells. As can be seen from the side views in Figs. 1(e) and 1(f), the SW defects lead to vertical displacements of hundreds of atoms in a typical simulation cell. Similar buckled SW transformations are predicted for hexagonal boron-nitride (BN) and polycyclic aromatic hydrocarbons (PAHs) above a critical size, demonstrating the relevance of these results to sp^2-bonded materials in general. These results suggest that SW defects may enhance the tendency of graphitic layers to transform into nonplanar nanostructures such as nanotubes and fullerenes[18,19] and that SW defects may play a role in the intrinsic rumpling of graphene.

II. METHODS

The DFT calculations reported herein have been performed with the plane-wave code CPMD.[20] Troullier-Martins norm-conserving pseudopotentials[21] are employed with an energy cutoff of 100 Ry. A large variety of hexagonal and rectangular supercells was considered, ranging from a 5×5 hexagonal cell (50 atoms) to a 13×5 rectangular cell (260 atoms). Γ point sampling of the Brillouin zone was used throughout.[22] In most DFT calculations, the Perdew-Burke-Ernzerhof (PBE) (Ref. 23) exchange-correlation (xc) functional is employed. However, tests with local-density approximation (LDA) and the hybrid PBE0 (Ref. 24) xc functionals are also reported in Table I and discussed briefly below.

The periodic QMC calculations have been performed with the CASINO code,[25] using the diffusion Monte Carlo method[26] with the short-time approximation and a time step of 0.0125 a.u. A carbon Dirac-Fock pseudopotential,[27] with a frozen He core and 0.58 Å radius, was used. Trial wave functions were of the Slater-Jastrow type, with single-particle orbitals obtained from DFT-LDA calculations performed with the PWSCF code[28] using an energy cutoff of 300 Ry and re-expanded in B splines.[29] Further details of the setup can be found in Ref. 30.

III. RESULTS

Calculations of SW defects starting with all atoms in the same plane yield a flat SW defect structure, as reported
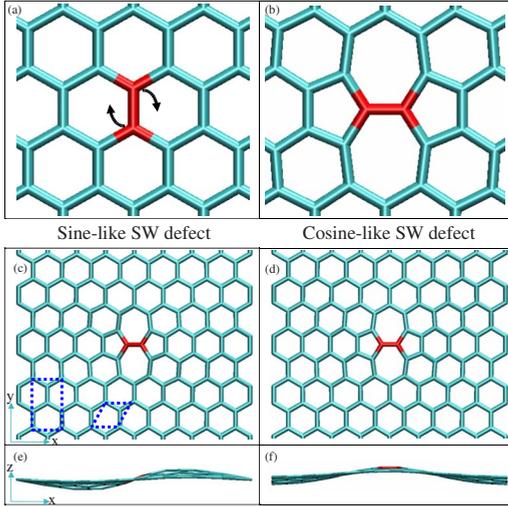
FIG. 1. (Color online) The structure of the flat and two buckled SW defects in graphene. (a) Top view of perfect graphene. (b) Top view of an unstable flat SW defect. (c) and (e) Top and side views of the sinelike buckled SW defect. (d) and (f) Top and side views of the cosinelike buckled SW defect. The rotated bonds at the defect core are highlighted. The sinelike defect is the most stable defect structure identified. In (c) 1×1 rectangular and hexagonal cells are indicated by the dashed lines.

TABLE I. Formation energies of flat (E_{fl}) and sinelike buckled (E_{bu}) SW defects and the formation energy differences ($\Delta E = E_{fl} - E_{bu}$) in various cells computed with DFT and QMC. The buckling height (h)(the difference along the z axis between the highest and lowest carbon atom in the supercell) is also reported.

	E_{fl} (eV)	E_{bu} (eV)	ΔE (meV)	h (Å)
PBE, (8×5)-rect	5.02	4.66	357	1.51
PBE, (10×5)-rect	4.93	4.66	273	1.62
PBE, (10×6)-rect	4.91	4.64	275	1.63
PBE, (11×5)-rect	4.90	4.61	289	1.67
PBE, (13×5)-rect	4.89	4.66	227	1.67
PBE, (5×5)-hex	5.53	5.26	269	1.16
PBE, (8×8)-hex	4.96	4.71	253	1.40
PBE, (11×11)-hex	4.82	4.59	231	1.61
LDA, (5×5)-hex	5.63	5.42	210	1.07
PBE0, (5×5)-hex	5.69	5.63	61	0.79
QMC, (5×5)-hex [a]	5.92 ± 0.03 [b]	5.82 ± 0.03	96 ± 20	
ZPE correction[c]	$+0.06$	-0.03	$+95$	

[a]PBE structure used.
[b]The statistical error is one standard deviation.
[c]Zero point energies (ZPEs) calculated with PBE in a 5×5 cell.

before.[16,17] A vibrational analysis of this structure, however, reveals that this standard defect structure is not a local minimum on the PES but instead has two imaginary frequencies. The imaginary frequencies lead to two buckled (i.e., out-of-plane) wavelike defect structures [Figs. 1(c)–1(f)]. In one structure the carbon atoms at the defect core (i.e., the rotated C-C bond) move out of plane along the z axis in the same direction [Fig. 1(f)]. In this case there is a maximum in carbon heights at the defect core, and thus in cross section (along the x axis) the buckling resembles a cosinelike wave. In the other defect structure the atoms at the defect core move out of plane in opposite directions. The wave changes sign at the defect core and so resembles a sinelike wave. This sinelike structure is a true minimum with no imaginary frequencies, whereas the cosinelike structure is a transition state with one imaginary frequency. The buckled structures that emerge involve displacements of most atoms in the supercell(s) including large vertical displacements parallel to the defect core: the height between the highest and lowest carbon atom being ~1.4 Å and ~1.7 Å for the cosine- and sinelike waves [Fig. 2(b)], respectively.

Let us now focus on the sinelike defect, which is the more stable of the two buckled structures and about 200 meV more stable with PBE than the canonical flat defect (Table I). We have carefully checked each of the issues that may affect the structure and relative stability of the sinelike defect. Specifically, calculations in a range of supercells have been performed, ZPEs and cell relaxations have been taken into account,[31] and tests with other DFT xc functionals (LDA and PBE0) and QMC have been performed. As can be seen from Fig. 2(b) and Table I, the buckling height and defect formation energy is quite well converged with respect to cell size once a 13×5 cell is reached. Moreover, with all functionals

and QMC the buckled sinelike defect is $\gtrsim 100$ meV more stable than the flat SW defect and ZPE corrections enhance this preference by a further ~100 meV. The absolute formation energy of the SW defects is also reported in Table I. Previous first-principles estimates of this value (for the flat SW defect) vary widely: from 4.8 to 10.4 eV.[16,17] This large range has emerged mainly because rather small supercells were used (e.g., 3×3 cell in (Ref. 17) or only partial geometry optimizations were performed (e.g. Ref. 16). Here we obtain a converged value with respect to cell size for PBE of ~4.7 eV. Taking the energy difference between PBE and QMC in the 5×5 cell and adding this to the converged PBE result in the 13×5 cell leads to the best estimate of the QMC defect formation energy of ~5 eV for the sinelike buckled defect.

We now discuss some of the signatures of the sinelike SW defect that may be observable in experiment. Already SW defects have been identified in graphene with transmission electron microscopy.[32] However, information about displacements out of plane was not obtained. A local scanning probe method such as scanning tunneling microscopy (STM) or atomic force microscopy may prove to be useful techniques to verify the predictions made here. Indeed the Tersoff-Hamann[33] STM simulation in Fig. 2(a) indicates that the buckling—considerably more pronounced than the buckled Moiré pattern observed with STM for graphene on, e.g., iridium[34]—should be clearly visible. However, we caution that the results obtained are likely to be sensitive to temperature because we find that the sinelike defect can readily flip (i.e., change phase) about the defect center, going through the cosinelike SW defect as a transition state. The zero-point energy corrected barrier for this process is around 200 meV, and the pre-exponential factor (obtained from the computed
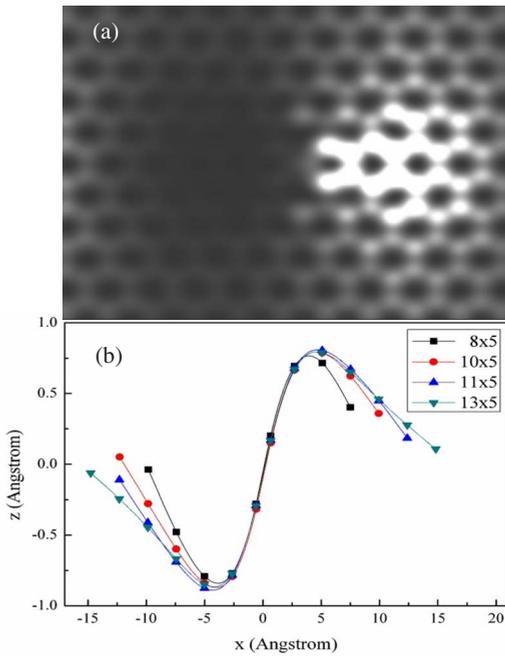
FIG. 2. (Color online) Simulated STM image and structural information of the sinelike buckled SW defect. (a) An example of a Tersoff-Hamann STM simulation in a 10×5 unit cell displaying occupied states within 1.5 eV of the Fermi level taken at 1.5 Å above the graphene sheet. (b) Dependence of the buckling height and the "wavelength" of the sinelike defect structure on the length of the supercell shown as a cross section along the x axis for the atoms in the interval $y \in [0, 1.5]$ Å.

harmonic vibrational frequencies) is 2×10^{12} s^{-1}. At cryogenic temperatures such as 70 K, the rate of flipping will be on the order of once per minute and should be sufficiently slow so that the buckled structure could be observed. Of course, this suggestion is reminiscent of the Si dimer on Si(100) discussion some years ago.[35–38] Vibrational spectroscopy is another technique with which the structure may be further characterized. The computed Γ point phonon frequencies of the flat and sinelike buckled defect structures exhibit differences from each other and from graphene. In particular the maximum phonon frequencies, corresponding to the stretch of the rotated C-C bond, for the flat and buckled SW structure are 1880 and 1774 cm^{-1}, respectively, well separated from each other and from the maximum computed frequency of perfect graphene (1612 cm^{-1}).

Let us now consider why the SW defect in graphene buckles and does not remain flat as previously assumed. The explanation we arrive at is simple and merely related to strain relief. In perfect graphene the equilibrium (PBE) C-C bond length is 1.42 Å. Upon making the flat SW defect, the C-C bond between the rotated atoms is compressed to 1.32 Å. Since in-plane motion of C atoms in graphene is much stiffer than out-of-plane motion, the flat structure cannot release the compression efficiently. To expand the compressed bond, the carbon atoms instead move out of plane. This out-of-plane motion at the immediate defect core "pulls" the neighboring atoms out of plane to ensure that the entire C-C bonding network remains as close to a planar
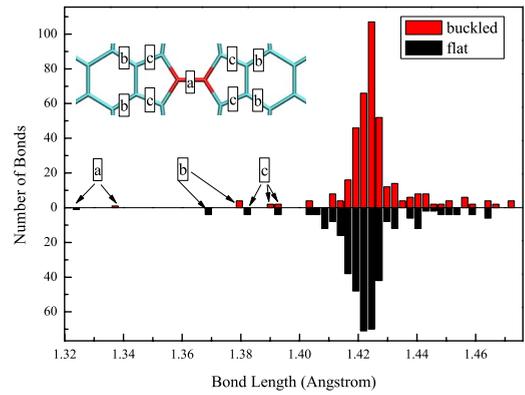
FIG. 3. (Color online) Histograms of C-C bond lengths for a flat (bottom) and a sinelike buckled (top) SW defect in graphene computed in a 13×5 rectangular cell. Through buckling to the sinelike structure many C-C bonds get slightly elongated. Some of the particular bonds that lengthen in the vicinity of the defect core are indicated with the help of the inset and labels.

sp^2-bonded network as possible. The strain relief achieved through the out-of-plane displacements can be directly seen from Fig. 3, which plots histograms of bond lengths for the flat and sinelike buckled structures. In the buckled defect the C-C bond at the defect core is ~0.01 Å longer than in the flat defect and, in addition, there are many more C-C bonds that are slightly elongated in the buckled compared to the flat defect structure (Fig. 3).

The explanation provided above is, of course, quite general, suggesting that buckling may stabilize SW defects in other planar sp^2 bonded materials. To test this we first examined a SW defect in a layer of hexagonal BN. In a 8×8 cell the sinelike SW defect is ca. 400 meV more stable than the flat SW defect, an even larger preference than the one obtained for graphene. Again through buckling the bonds around the dislocation core expand. Second, we extended the analysis to model PAHs in order to determine the cluster size dependence of buckling in SW defects. To this end we examined several series of fused aromatic rings ranging from the smallest molecular analog of a SW defect, azupyrene ($C_{16}H_{10}$), to one-dimensional (1D) tapelike clusters up to $C_{50}H_{28}$, to two-dimensional planar clusters up to $C_{228}H_{38}$. These studies show, as is known already, that azupyrene is planar. More importantly they predict that none of the 1D (one benzene wide) clusters exhibit a tendency to buckle. This is because the strain induced through creation of the SW defect can be released by expansion parallel to the rotated C-C defect core. Indeed the equilibrium C-C bond at the center of azupyrene is at 1.38 Å, significantly longer than the 1.32–1.33 Å of the C-C bonds in the graphene SW defect cores. However, as the planar clusters are extended in two dimensions and the lateral expansion becomes progressively more difficult due to the presence of additional C-C bonds perpendicular to the defect, eventually the clusters exhibit a tendency to buckle upon the creation of SW defects. The onset of buckling occurs once the planar clusters become about 3 nm wide in each direction. Specifically, for a 2D symmetric $C_{228}H_{38}$ cluster with a SW defect at its center the sinelike buckled structure becomes more stable than the

flat SW defect by ~ 10 meV with out-of-plane displacements on the order of 0.1 Å. We anticipate that as the clusters are increased in size in each dimension and become more representative of graphene flakes and nanoribbons, the tendency for the SW defects to buckle will steadily increase. Exploring this dependence in detail, beyond the ~ 300 atom limit of our current computational resources, will likely provide interesting work for the future.

IV. CONCLUSIONS

In conclusion, based on the results of DFT and QMC, we suggest that SW defects in graphene are more complex and interesting than hitherto appreciated. They are not simple 2D defects but rather involve large out-of-plane displacements of the atoms in the immediate vicinity of the defect that set up long-range out-of-plane displacement fields. This conclusion can also be generalized to hexagonal BN and PAHs beyond a critical size.

It remains to be seen if the predictions made here can be verified experimentally, although we have discussed some of the signatures of the buckled structure that could be detected with, e.g., STM and vibrational spectroscopy. We note, however, that the large value of the absolute formation energy of SW defects (ca. 5 eV) implies that the equilibrium concentration of SW defects in graphene at room temperature will be exceedingly small. SW defects are only likely to be present and detectable in graphene under nonequilibrium conditions or when formed through irradiation or the effects of mechanical strain.

Finally, in a more general context the results reported here are another illustration that layered sp^2-bonded materials are highly susceptible to buckling and that SW defects should enhance the tendency of graphitic layers to roll up into other carbon nanostructures such as nanotubes and fullerenes.[18,19] SW defects may also play a role in the intrinsic rumpling of graphene.

*angelos.michaelides@ucl.ac.uk
[1] A. J. Stone and D. J. Wales, Chem. Phys. Lett. **128**, 501 (1986).
[2] B. R. Eggen et al., Science **272**, 87 (1996).
[3] C. P. Ewels et al., Chem. Phys. Lett. **351**, 178 (2002).
[4] M. Buongiorno Nardelli et al., Phys. Rev. Lett. **81**, 4656 (1998).
[5] M. Buongiorno Nardelli et al., Phys. Rev. B **57**, R4277 (1998).
[6] G. G. Samsonidze et al., Phys. Rev. Lett. **88**, 065501 (2002).
[7] J. Kang et al., Phys. Rev. B **77**, 115453 (2008).
[8] J. M. Carlsson and M. Scheffler, Phys. Rev. Lett. **96**, 046806 (2006).
[9] D. W. Boukhvalov and M. I. Katsnelson, Nano Lett. **8**, 4373 (2008).
[10] E. J. Duplock et al., Phys. Rev. Lett. **92**, 225502 (2004).
[11] F. OuYang et al., J. Phys. Chem. C **112**, 12003 (2008).
[12] H. Terrones and A. L. Mackay, Carbon **30**, 1251 (1992).
[13] G. Csányi et al., Phys. Rev. B **75**, 085432 (2007).
[14] M. T. Lusk and L. D. Carr, Phys. Rev. Lett. **100**, 175503 (2008).
[15] H. Amara et al., Phys. Rev. B **76**, 115423 (2007).
[16] E. Kaxiras and K. C. Pandey, Phys. Rev. Lett. **61**, 2693 (1988).
[17] L. Li et al., Phys. Rev. B **72**, 184109 (2005).
[18] D. Ugarte, Nature (London) **359**, 707 (1992).
[19] I. V. Lebedeva et al., Physica E (Amsterdam) **40**, 2589 (2008).
[20] J. Hutter et al., computer code CPMD, version 3.11 (copyright IBM Corp. 1990–2006; copyright für Festkörperforschung Stuttgart, Germany, 1997–2001), http://www.cpmd.org/
[21] N. Troullier and J. L. Martins, Phys. Rev. B **43**, 1993 (1991).
[22] K-point convergence tests were performed in a 7×7 hexagonal cell with $2 \times 2 \times 1$ k points and an 8×5 rectangular cell with $5 \times 5 \times 1$ k points. The energy difference between the structures of interest (i.e., the flat and sinelike SW defects) change by ≤ 30 meV compared to the Γ point results reported.
[23] J. P. Perdew et al., Phys. Rev. Lett. **77**, 3865 (1996).
[24] C. Adamo and V. Barone, J. Chem. Phys. **110**, 6158 (1999).
[25] R. J. Needs et al., CASINO Version 2.1 User Manual (University of Cambridge, Cambridge, 2007).
[26] W. M. C. Foulkes et al., Rev. Mod. Phys. **73**, 33 (2001).
[27] J. R. Trail and R. J. Needs, J. Chem. Phys. **122**, 014112 (2005); **122**, 174109 (2005); see also www.tcm.phys.ac.uk/~mdt26/casino2_pseudopotentials.html
[28] S. Baroni et al., http://www.pwscf.org
[29] D. Alfè and M. J. Gillan, Phys. Rev. B **70**, 161101(R) (2004).
[30] J. Ma et al., J. Chem. Phys. **130**, 154303 (2009).
[31] The influence of cell relaxations was carefully examined in a number of supercells. For example, in a 10×5 rectangular cell with PBE the sinelike buckled structure is 130 (260) meV more stable than the flat defect after (before) relaxation. Upon relaxation the cell expands parallel to the rotated bond (x axis) by 0.6 and 0.2% and shrinks perpendicular to it (y axis) by 0.4 and 0.5% for the flat and sinelike buckled structure, respectively.
[32] J. C. Meyer et al., Nano Lett. **8**, 3582 (2008).
[33] J. Tersoff and D. R. Hamann, Phys. Rev. Lett. **50**, 1998 (1983).
[34] A. T. N'Diaye, S. Bleikamp, P. J. Feibelman, and T. Michely, Phys. Rev. Lett. **97**, 215501 (2006).
[35] T. Uda, H. Shigekawa, Y. Sugawara, S. Mizuno, H. Tochihara, T. Yamashita, J. Yoshinobu, K. Nakatsuji, H. Kawai, and F. Komori, Prog. Surf. Sci. **76**, 147 (2004).
[36] J. Dąbrowski and M. Scheffler, Appl. Surf. Sci. **56-58**, 15 (1992).
[37] T. Yokoyama and K. Takayanagi, Phys. Rev. B **61**, R5078 (2000).
[38] Y. Kondo, T. Amakusa, M. Iwatsuki, and H. Tokumoto, Surf. Sci. **453**, L318 (2000).